Control of cardiac function and noise from a decaying power spectrum

G. C. Kember,[1] J. A. Armour,[2] G. A. Fenton,[1] and A. Malhotra[1]
[1]*Department of Engineering Mathematics, Dalhousie University, P. O. Box 1000, Halifax, Nova Scotia, Canada, B3J 2X4*
[2]*Department of Pharmacology, University of Montreal, Montreal, Quebec, Canada H3C 3J7*
(Received 20 June 2003; revised manuscript received 26 February 2004; published 23 August 2004)

Evidence is presented that adds to the debate surrounding the question: To what extent does neural control of cardiac output exploit noise? The transduction capability of cardiac afferent neurons, situated in and adjacent to the heart, is vital to feedback in control of cardiac function. An analysis of *in situ* cardiac afferent activity shows evidence of independent and exponentially distributed interspike intervals. An anatomical basis for such memoryless interspike intervals ultimately derives from the fact that each afferent neuron is associated with a field of sensory neurites, or bare nerve endings, that transduce local chemical and mechanical stimuli in a many-to-one fashion. As such, cardiac afferent neurons and their sensory neurite inputs are respectively modeled here by the Hodgkin–Huxley equations forced by "red" noise (decaying power spectrum) perturbing an otherwise constant subthreshold input. A variable barrier competition model is derived from these equations in order to address the question: How are noisy inputs being processed by sensory neurons to cause each spike? It is found that ion channels are responsible for significant input "whitening" (increased spectral power at higher frequency) through differentiation of the inputs. Such whitening is a means to distinguish low-frequency control signals from otherwise red noise fluctuations. Furthermore, spiking occurs when backward moving averages of the whitened inputs, over a window of the order of the sodium activation time scale, exceed an approximately constant barrier.

DOI: 10.1103/PhysRevE.70.021909 PACS number(s): 87.19.Hh, 05.40.−a

I. INTRODUCTION

Stochastic resonance (SR) is said to occur when a certain level of noise enhances the response of a nonlinear system to low amplitude, *periodic* signals. An introduction to SR and a summary of the earlier literature is available in Ref. [1] while a later review may be found in Ref. [2]. Aperiodic stochastic resonance (ASR) is a generalization of SR to the study of noise enhancement of a nonlinear system's response to *aperiodic* inputs [3]. In previous studies, energy models have been used to approximate the system dynamics and allow the development of measures for information throughput. For example, ASR in sensory neurons has been described using the correlation between noisy subthreshold inputs and the average activity level generated by such neurons [3–5]. With respect to SR, measures of the response of sensory neurons subjected to noisy periodic inputs have been represented in terms of the relationship between the input power spectrum and the same constructed for the average firing rate [6–8]. Measures of information throughput, as described above, do not involve the modeling of a mechanism by which each spike (action potential) is produced in response to noisy external inputs. As such, they give a "black-box" description of the relationship between the noisy inputs and their effect on the neural firing patterns. Therefore, in this paper, a causal relationship is found that links the inputs with the outputs (action potentials or "spikes") to better understand *how* noisy inputs are processed in the Hodgkin–Huxley (HH) equations to produce each spike. The application is cardiac control and this is described first.

Feedback of heart status to the entire cardiac neuronal hierarchy is derived from cardiac afferent neurons with sensory neurite fields in various regions of the heart and major intrathoracic vessels. These sensory neurite fields constantly transduce the local mechanical and chemical state of divergent regions of the heart. Many studies have been focussed on the 10% [9] of cardiac afferent neurons that generate activities relatively phase-locked to beat-to-beat cardiac mechanical events ([10–13]). These rapidly transducing, or "fast-responding" (within the time scale of a beat), afferent neurons may be primarily involved in control of heart rate and coordinating regional cardiac mechanics on a beat-to-beat basis. However, the majority of cardiac afferent neurons identified in the cardiac neuronal hierarchy generate activity that bears little direct relationship to regional cardiac mechanical events. As such their activity is not reflective, for example, of blood pressure generation. These neurons, referred to from hereon as "slow-responding" (over the timescale of many beats) neurons, show sporadic activity with average firing rates that are typically in the 0.1–1 Hz range, e.g. Ref. [14]. To date there have been few experimental or theoretical studies concerning the transduction characteristics of these slow-responding cardiac afferent neurons. In fact, their role in cardiac control remains an open question.

Anatomical evidence is accumulating that slow-responding cardiac afferent neurons are key to providing feedback to the entire cardiac neuronal hierarchy over many cardiac cycles, reflective of chemosensory transduction over longer times [15]. This contrasts with the idea that fast-responding reflex control within medullary neurons may not only be involved in control over relatively short (single beat) time scales but also longer time scales via scaling properties of their interspike intervals [16]. However, the anatomical evidence allows another possibility; longer-term control is physically distinct from shorter term control, in that the latter mainly relates to cardiac mechanical events while the former is primarily driven by inputs from slow-responding cardiac afferent neurons. The following are some features of the

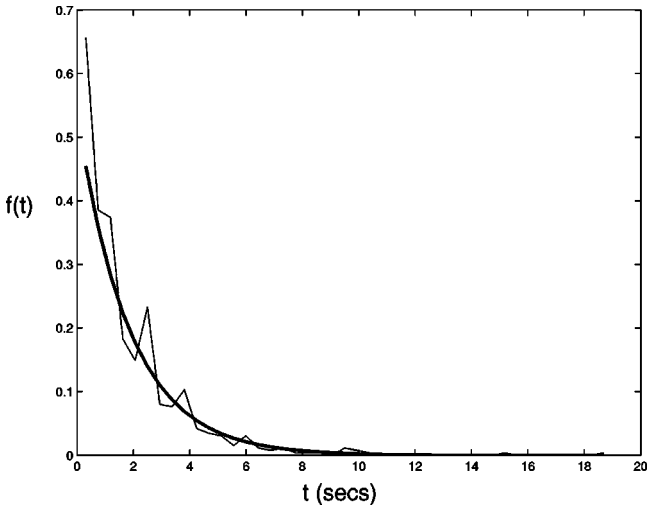

FIG. 1. Histogram comparing experimental (lighter line) and exponential [$f(t)=\lambda \exp(-\lambda t)$, shown as heavier line] probability density distributions of interspike intervals. The neural data [14] was discriminated for spikes where spikes were assumed to occur at voltage peaks exceeding 0.2 mV that were also separated by at least 20 ms (maximal firing rate of 50 Hz) from a previous spike.

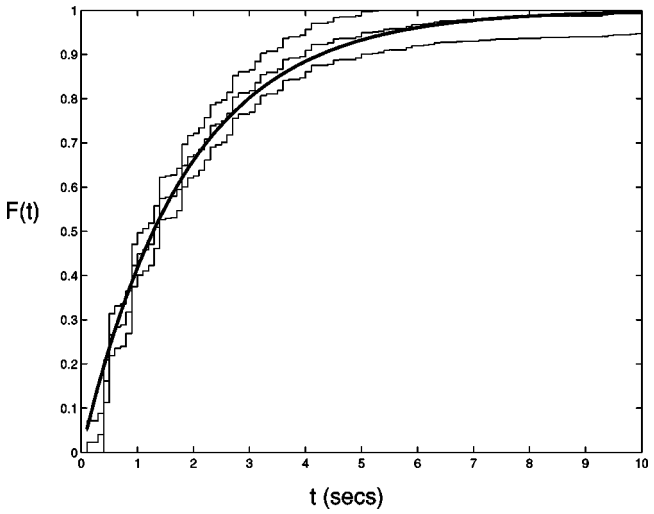

FIG. 2. Comparison of cumulative distributions of interspike intervals from the exponential distribution, i.e., $F(t)=1-\exp(-\lambda t)$ shown as the heavier line, and the same computed from the data using the KS statistic. The 90% confidence limits are also depicted. The experimental and theoretical results are very close. However, as expected, they are in disagreement at interspike intervals less than the typical time between heart beats (the canine heart rate was steady in this protocol [14] with 0.5 s between beats).

slow-responding neurons: (i) Their interspike intervals (time between action potentials) are aperiodic, (ii) the average time between action potentials is the order of 1 s or longer during normal states ([17,18]), (iii) they are required for maintenance of autonomic efferent (feedforward) neuronal outputs that affect cardiac contractility over time scales encompassing many cardiac cycles ("slow" or "long" time scales ranging over 1–30 min) [9], (iv) their somata (cell bodies) are part of a distributed network that feed back heart status to spinal cord neurons [19], brain stem [20] within the central nervous system, and intrathoracic ganglia [9] that ultimately control cardiac efferent neuronal behavior, and (v) they each receive inputs from vast fields of bare nerve endings (or "sensory neurites"), that are usually located in relatively confined epicardial, myocardial, and endocardial regions where they transduce the local mechanical and chemical environments [21].

Evidence of exponentially distributed interspike intervals is provided from a 20 min 10 kHz recording of canine intrinsic cardiac neurons associated with sensory neurites located in the right atrium of the canine heart. These data were studied in another context in Ref. [14] and were taken during control states from an anaesthetized canine preparation. The 20 min of data were "discriminated" (Fig. 1 caption) to identify spikes and the interspike interval histogram appears to approximate an exponential distribution. A further comparison of the cumulative distribution function of the data with the exponential distribution, as represented by the Kolmogorov–Smirnov ("KS") test, is shown in Fig. 2 along with 90% confidence intervals. The KS and its confidence intervals indicate that the empirical and theoretical cumulative functions are in close agreement. A useful feature of the KS plot is that it also shows the effect of mechanical transduction due to cardiac mechanics. Specifically, the empirical and fitted distributions begin to deviate for interspike intervals at or below about 0.5 s which is approximately the average time between heart beats in this *in situ* experimental protocol. In summary, the observation of exponentially distributed interspike intervals is unsurprising given that the vast array of sensory neurites associated with an individual cardiac afferent neuron represents a many-to-one transduction scheme [19,22].

Cardiac sensory neurites are capable of transducing the local chemical and/or mechanical state in selective cardiac regions ([10–12,23]). Gradual changes in the chemical state of the heart are reflected as a slowly varying aperiodic control signal where spike trains are not observed. On the other hand, the mechanical state represents local distortion of muscle fasicles in any given region of the heart that are sensed as fast fluctuations by mechanosensory neurites ([19], [24]). The simplest model for sensory inputs to a slow-responding cardiac afferent neuron from their arrays of sensory neurites is a slowly varying aperiodic chemical control signal perturbed by an additive mechanically derived noisy signal [19]. The noisy signal is assumed here to have a decaying, or "red", power spectrum. This assumption is physically reasonable in that it ensures that the noise possesses a finite variance, in contrast to "white" noise having a flat power spectrum, while details of the noise distribution must await further experimentation.

The HH equations are used as a model of slow-responding cardiac afferent neurons. The HH equations are reasonable to the extent that cardiac afferent neurons do fire repetitively in response to a constant, and sustained input that exceeds a threshold. Further, the rate of spiking increases as the sustained input level is increased [17]. However, the HH equations are unreasonable at very high inputs since their activity becomes suppressed. Activity generated,

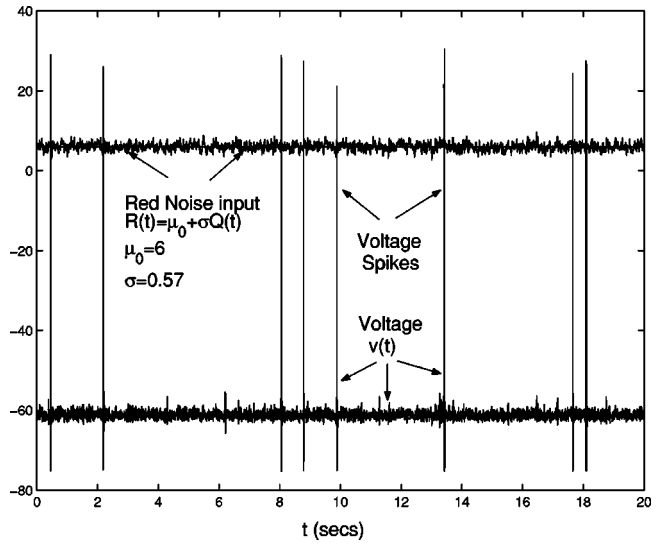

FIG. 3. The numerical solution of the HH equation (2), shown along with red noise inputs $R(t)=\mu_0+\sigma Q(t)$, where $\mu_0=6$ is the expected value of $R(t)$ and the red noise standard deviation is $\sigma=0.57$ (Sec. III). The solution is initialized at the stable steady state associated with $\mu_0=6$. Since the sustained input level at which the steady-state solution becomes unstable and undergoes a Hopf bifurcation is $\mu_0\approx 9.8$, the sustained input, $\mu_0=6$, is a subthreshold input that elicits no spiking. The red noise fluctuations, $\sigma Q(t)$, perturbing the subthreshold input level, $\mu_0=6$, are responsible for observed spiking. Note, in the absence of firing, the voltage variable $v(t)$ fluctuates near, and around, the stable steady state $v_0\approx -63.5$.

in vivo, by a cardiac afferent neuron stays at maximal firing rates when exposed to further increases in a chemical stimulus [17]. Since such high sustained inputs are much greater than those where constant firing commences, this contrasting behavior is disregarded here.

It is important to clarify the noise-processing regime of the HH equations considered here. The slowly varying aperiodic input, the chemical control signal, is assumed to lead to a persistent and slowly varying subthreshold depolarization above the resting voltage. The term "subthreshold" implies that no spiking occurs in response to the chemical control signal on its own. A piecewise constant approximation of the control signal is made to simplify its analysis to the independent consideration of constant sustained inputs as seen in Fig. 3 (Sec. III). Given that the control signal produces a subthreshold variation away from the rest voltage, it is the additive noise perturbing the piecewise constant control signal that becomes necessary to initiate spiking. The linear combination of the sustained, but subthreshold, input and additive noise is also assumed primarily to lead to the generation of *isolated* spikes (not spike trains) as seen in cardiac preparations, e.g. Ref. [14].

Given the above discussion, the voltage response of the HH equations (Sec. II) to red noise inputs, perturbing a constant subthreshold input that would cause no response in the absence of the noise, is considered. An example with approximately exponentially distributed interspike intervals (Sec. III) is provided in Fig. 3. The question considered here is: "How are noisy inputs being processed to cause each spike?" This question is explored using a variable barrier competition model (Sec. IV) derived from the HH equations (Sec. II). The competition variable barrier model is approximated as a constant barrier energy model (Sec. V). A discussion of control of cardiac output coming from the competition model is given in Sec. VI.

II. EFFECTIVE STEP INPUT

An "effective" input to the HH equations is first derived from its linearized form and termed the "coupled" linearized form since it involves the voltage variable and ion channel variables. The coupled linearized form is modified to an "uncoupled" linearized form where the ion channel variables have been eliminated. This results in a linearized form where the voltage is the sole dependent variable and the ion channel variables have been exchanged for an external forcing equal to a linear combination of the original external input and its derivatives up to third order. This latter input is termed the effective input. In other words, the removal of the ion channel variables links the dependence of the voltage response in the coupled linearized form, and thus approximately the HH equations, to external input fluctuations. This effective input is then used to construct an "effective step" input to the HH equations. The response to the effective step input is linked to the Hopf bifurcation of the steady state in response to a sustained input.

A. Coupled form of linearized Hodgkin–Huxley equations

The HH equations [25] are

$$C\dot{v} = -g_{\mathrm{Na}}m^3h(v-v_{\mathrm{Na}}) - g_{\mathrm{K}}n^4(v-v_{\mathrm{K}}) - g_L(v-v_L) + R(t),$$

$$\dot{m} = a_m'(v)(1-m) - b_m'(v)m,$$

$$\dot{h} = a_h'(v)(1-h) - b_h'(v)h,$$

$$\dot{n} = a_n'(v)(1-n) - b_n'(v)n, \tag{1}$$

where $R(t)$ is an external input and

$$a_m'(v) = \frac{0.1(v+40)}{1-\exp[-(v+40)/10]},$$

$$b_m'(v) = 4\,\exp[-(v+65)/80],$$

$$a_h'(v) = 0.07\,\exp[-(v+65)/20],$$

$$b_h'(v) = \frac{1}{1+\exp[-(v+35)/10]},$$

$$a_n'(v) = \frac{0.01(v+55)}{1-\exp[-(v+55)/10]},$$

$$b_n'(v) = 4\,\exp[-(v+65)/80].$$

The constant parameters are chosen as [25]: $C=1\ \mu\mathrm{F/cm^2}$, $v_L=-54.4$ mV, $g_L=0.3\ \mathrm{mS/cm^2}$, $v_{\mathrm{K}}=-77$ mV, g_{K}

$=36\ \mathrm{mS/cm^2}$, $v_{\mathrm{Na}}=50$ mV, and $g_{\mathrm{Na}}=120\ \mathrm{mS/cm^2}$.

The HH equation (2) may be formally restated as

$$C\dot{v} = f(v,m,h,n) + R(t),$$

$$\dot{m} = g_m(m,v),$$

$$\dot{h} = g_h(h,v),$$

$$\dot{n} = g_n(n,v). \tag{2}$$

The stable steady state, in response to a constant external input $R(t)=\mu_0$, is denoted by $(v,m,h,n)=(v_0,m_0,h_0,n_0)$. The solution of the HH equations, forced by time dependent $R(t)=\mu_0+\epsilon Z(t)$, is written as $v(t)=v_0+\epsilon V(t)$, $m(t)=m_0+\epsilon M(t)$, $h(t)=h_0+\epsilon H(t)$, $n(t)=n_0+\epsilon N(t)$ and ϵ is a constant scaling. If the solution $(v(t),m(t),h(t),n(t))$ remains close to (v_0,m_0,h_0,n_0) in response to $R(t)=\mu_0+\epsilon Z(t)$, then $(V(t),M(t),H(t),N(t))$ approximately satisfies the linearized form of the HH equations, i.e.,

$$\dot{V} = c_v V + c_n N + c_m M + c_h H + Z(t),$$

$$\dot{M} = -a_m M + b_m V,$$

$$\dot{H} = -a_h H + b_h V,$$

$$\dot{N} = -a_n N + b_n V, \tag{3}$$

with three sets of constants: (i) The rate constants a_x equal to the minus partial derivatives of g_x with respect to x (x is one of m, n, or h), (ii) the constants b_x which are the partial derivatives of g_x with respect to the voltage v (x is one of m, n, or h), and (iii) the constants c_x, x is one of v,m,h, or n are equal to the partial derivatives of $f(v,m,h,n)$ with respect to the variables v, m, h, and n respectively, and all of the above derivatives are evaluated at the stable fixed point solution (v_0,m_0,h_0,n_0).

B. Effective input

The ion channel variable perturbations $M(t)$, $H(t)$, and $N(t)$ in Eq. (3) are eliminated to expose the dependence of the perturbation voltage $V(t)$ upon fluctuations in the external input $Z(t)$ fed back by the ion channels. This elimination is simplified by using the Laplace transform of Eq. (3) subject to zero-initial conditions (for algebraic convenience and without loss of generality). If s is the Laplace transform variable, and $\tilde{V}(s)$, $\tilde{M}(s)$, $\tilde{H}(s)$, $\tilde{N}(s)$, and $\tilde{Z}(s)$ are the respective Laplace transformations of $V(t)$, $M(t)$, $H(t)$, $N(t)$, and $Z(t)$ then

$$\begin{bmatrix} s+a_v & -b_v & -c_v & -d_v \\ -b_m & 0 & s+a_m & 0 \\ -b_h & 0 & 0 & s+a_h \\ -b_n & s+a_n & 0 & 0 \end{bmatrix} \begin{bmatrix} \tilde{V}(s) \\ \tilde{M}(s) \\ \tilde{H}(s) \\ \tilde{N}(s) \end{bmatrix} = \begin{bmatrix} \tilde{Z}(s) \\ 0 \\ 0 \\ 0 \end{bmatrix}. \tag{4}$$

Solving for $\tilde{V}(s)$ gives the decoupled form

$$[(s+a_v)(s+a_m)(s+a_n)(s+a_h) + b_v(s+a_m)(s+a_n) - c_v b_m(s+a_h) + d_v b_h(s+a_m)]\tilde{V}(s) = (s+a_n)(s+a_m)(s+a_h)\tilde{Z}(s). \tag{5}$$

Since the inverse transform of $s^n F(s)$, $n=0,1,\ldots$ equals $d^n f(t)/dt^n$ and it was assumed above that the lower-order derivatives and $f(t)$ evaluated at $t=0$ vanish, Eq. (6) inverts to

$$G[V(t)] = L[Z(t)], \tag{6}$$

where

$$G[V(t)] = \dddot{V}(t) + A_3\dddot{V}(t) + A_2\ddot{V}(t) + A_1\dot{V}(t) + A_0 V(t), \tag{7}$$

and the coefficients A_n, $n=0,1,2,3$ are, respectively, equal to the coefficients of s^n, $n=0,1,2,3$, while

$$L[Z(t)] = \dddot{Z}(t) + (a_m + a_h + a_n)\ddot{Z}(t) + (a_m a_n + a_h a_m + a_n a_h)\dot{Z}(t) + a_m a_n a_h Z(t). \tag{8}$$

It is clear that an input $L[Z(t)]$ to the uncoupled linearized form of the HH equations (6) corresponds to the coupled form (3) being forced by $Z(t)$. For example, the solution of $G[V]=L[Z]$ subject to zero-initial conditions on $V(t)$ and $Z(t)$, is identical to the solution of the coupled linearized form in Eq. (3) forced by $Z(t)$, where $Z(t)$ and $(V(t),M(t),H(t),N(t))$ also satisfy zero initial conditions. With respect to the voltage variable, the input $Z(t)$ to the coupled form (3) corresponds to an effective input $L[Z(t)]$ to the uncoupled form (6).[1]

The uncoupled form $G[V]=L[Z]$, based on Eqs. (7) and (8), provides an explicit dependence of the voltage variable on external input fluctuations that is otherwise implicit in the coupled formulation (3) involving the ion channel variables. This explicit dependence is necessary in the formulation of the competition model (Sec. IV).

C. Effective step input

An approximation to an effective step input is defined here via the uncoupled, linearized form $G[V]=L[Z]$. The voltage $v(t)$ is initialized at the stable fixed point solution

[1]Consider the coupled form $\dot{x}=y+t$ and $\dot{y}=-x$ subject to zero initial conditions. This is equivalent to the uncoupled form $\ddot{x}+x=1$ again subject to zero initial conditions. Thus the time dependent input, t, applied to the coupled form is an 'effective' step input applied at $t=0$ to the uncoupled form.

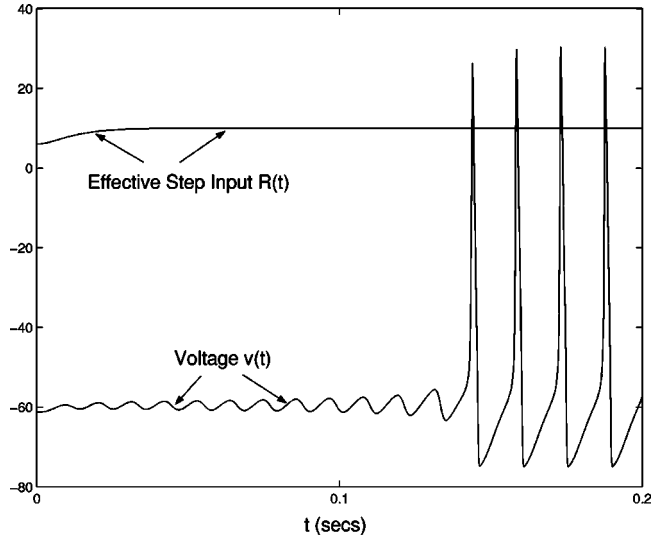

FIG. 4. Spiking eventually occurs in response to the effective step input $R(t)=\mu_0+Z(t)$. The effective step component, $Z(t)$, taken from the solution of $L[Z]=a_m a_h a_n(\mu^*-\mu_0)$, $a_m a_h a_n \approx 0.1$, $\mu_0=6$, $\mu^*=9.8$, and zero initial conditions, is applied to the HH equation (2). Spiking is observed when μ^* is increased beyond 9.8. The effective step input, $R(t)$, must be maintained long enough for a spike to be observed; spiking is not observed if μ^* is reset back to μ_0 before the occurence of a first spike.

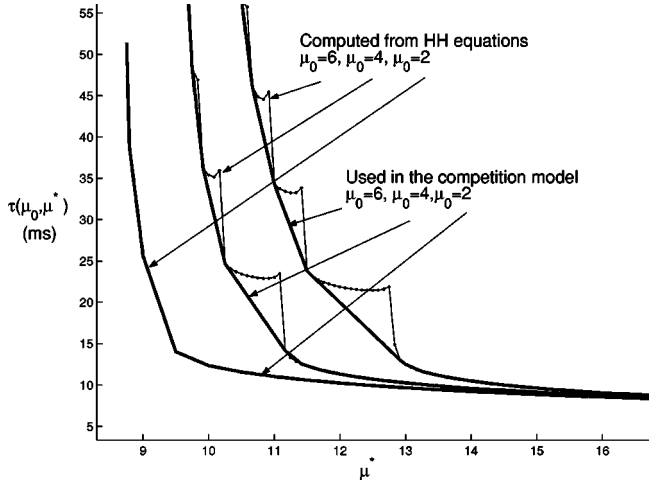

FIG. 5. The time to first spike curves are shown for $\mu_0=(2,4,6)$ where μ^* exceeds 9.8 (Sec. II). The time to a first spike is reduced as μ^* is increased. The minimum value of μ^* where spiking begins, approaches the Hopf bifurcation level $\mu^* \approx 9.8$ as μ_0 is increased.

associated with the constant external input μ_0 so that $(v(0),m(0),h(0),n(0))=(v_0,m_0,h_0,n_0)$. The scaling ϵ is set to unity giving $R(t)=\mu_0+Z(t)$, where it is also assumed that $R(0)=\mu_0$ or $Z(0)=0$. A step-input $L[Z(t)]=a_m a_n a_h(\mu^*-\mu_0)$ is then applied to Eq. (6) at $t=0$. The input $R(t)=\mu_0+Z(t)$, is thus termed an effective step input since the corresponding input to the coupled linearized form or the HH equations, is the *time-varying* input $R(t)$.[1] Note that $R(t)$ eventually reaches $R(\infty)=\mu^*$, since $Z(\infty)=\mu^*-\mu_0$. The response of the HH equations to an effective step input is shown in Fig. 4 with $\mu_0=6$ and $\mu^*=9.8$. The voltage variable qualitatively exhibits a Hopf bifurcation in that an unstable oscillation appears immediately after application of the effective step input $R(t)$ at $t=0$. This response can be understood from the linearized form of the HH equations in the following way. A Hopf bifurcation of the HH equations occurs for a constant external input $R(t) \approx 9.8$. A Hopf bifurcation of the uncoupled linear operator G *also* occurs near $\mu^*=9.8$ because the coefficients of G, i.e., A_i, $i=1,2,3,4$, depend upon the steady-state voltage which is equal to the initial condition, v_0, *augmented* by the steady-state response to the step input, i.e., the steady state is $v_0+a_m a_h a_n(\mu^*-\mu_0)/A_0$. Since this constant steady-state response linearly approximates the steady state of the HH equations in response to a constant input μ^*, spiking is eventually observed in response to an effective step input $R(t)$ when $\mu^* \approx 9.8$. The effective step input must be maintained "long enough" for spiking to be eventually observed in the HH equation (2) forced by $R(t)$ as in Fig. 4. Long enough means, for example, that if μ^* is back to $\mu_0<9.8$ some time after $t=0$ and before a first spike occurs, then spiking is not observed. It also follows that the time to a first spike, $\tau(\mu_0,\mu^*)$, generally decreases as μ^* increases beyond $\mu^* \approx 9.8$. The time to first spike in the HH equations, in response to $R(t)=\mu_0+Z(t)$ where $L[Z(t)]=a_m a_n a_h(\mu^*-\mu_0)$ with zero conditions on $Z(t)$, and $(v,m,h,n)=(v_0,m_0,h_0,n_0)$ is depicted in Fig. 5 for $\mu_0=(2,4,6)$ over a range of μ^*.

III. NOISY INPUTS

The external input, $R(t)$, to the HH equation (2) is now allowed to be the sum of a slowly varying aperiodic control signal $\mu(t)$ and noisy fluctuations $Z(t)=\sigma Q(t)$ (ϵ is redefined as σ) with zero mean and standard deviation σ. It is assumed that the control input $\mu(t)$ does not elicit spiking in the absence of $Z(t)$. A piecewise constant approximation is made to the slower control component $\mu(t)$, i.e.,

$$\mu(t)=\sum_{i=0}^{\infty}\mu_i[U(t-t_i)-U(t-t_{i+1})], \tag{9}$$

where $U(t)=0$, $t<0$, $U(t)=1$, $t\geqslant 0$, is the Heaviside step function. The times $(t_{i+1}-t_i)$ are assumed to be long enough that the mean spiking rate in response to $\mu_i(t_{i+1}-t_i)$ can be observed with sufficient accuracy. The change in levels between μ_i and μ_{i+1} is also small enough that spike trains are not provoked and the response to the sustained inputs μ_i, $i=0,1,2,\ldots$ may be independently considered. The i subscript notation is reduced to $i=0$ for convenience and $R(t)=\mu_0+\sigma Q(t)$, where μ_0 allows a natural reference to the discussion in the previous section.

The fluctuations $Q(t)$ form the red noise component of external forcing. The red noises are derived from the solution of $L[Q(t)]=S(t)$ where $S(t)$ is "almost" white noise taken from a stationary Gaussian random process with zero mean, unit variance, and exponentially decaying correlation function $\rho(\tau)=\exp\{-2|\tau|/\theta\}$. The correlation scale of fluctuation [26] $\theta=0.5$ ms is small and on the order of the spike rise

time so that $S(t)$ is approximately a band-limited white noise with finite variance. With respect to the linearized form (6), the almost white noise fluctuations $S(t)$ driving $G[V]$ (6), are equivalent to the red noise fluctuations, $Q(t)$, forcing the coupled, linearized form (3). With reference to the previous section, the $S(t)$ are effective almost white noise inputs. The spectral density functions of $Q(t)$ and $S(t)$, respectively, $S_Q(\omega)$ and $S_S(\omega)$, are related through

$$S_S(\omega) = |H_S(\omega)|^2 S_Q(\omega), \tag{10}$$

where

$$|H_S(\omega)| = \sqrt{(a_m^2+\omega^2)(a_n^2+\omega^2)(a_h^2+\omega^2)}. \tag{11}$$

Hence, red noise input fluctuations, $Q(t)$, are "whitened" by the differential operator L since increased circular frequency ω corresponds to increased $|H_S(\omega)|$. The physiological implication is that red noise fluctuations $Q(t)$ are being whitened by the recovery variables M, H, and N as approximated by the operations in the differential operator L.

IV. COMPETITION MODEL

The hypothesis made here is that the averaged response of the HH equations to the noisy inputs $R(t)=\mu_0+\sigma Q(t)$ (Sec. III) can be linked to their response to noiseless effective step inputs $R(t)=\mu_0+Z(t)$ (Sec. II). First, the backward local average of $v(t)$ is defined as

$$v_W(t) = \frac{1}{W}\int_{t-W}^{t} v(\xi)d\xi. \tag{12}$$

Second, if $v(t)$ is near the stable fixed point and not spiking, (Fig. 3) and $f_W(v,n,m,h) \approx f(v_W,n_W,m_W,h_W)$ [similarly for $g_x(x,v)$, x is m, h, or n] (2) then a first-order approximation to the backward averaged HH equations is

$$\dot{v}_W = f(v_W,m_W,h_W,n_W) + R_W(t),$$

$$\dot{m}_W = g_m(m_W,v_W),$$

$$\dot{h}_W = g_h(h_W,v_W), \tag{13}$$

$$\dot{n}_W = g_n(n_W,v_W), \tag{14}$$

which recovers the original HH equation (2). The noisy inputs are $R(t)=\mu_0+\sigma Q(t)$, where $L[Q]=S(t)$ and the fluctuations $S(t)$ are nearly white noises (Sec. III). Elimination of $Q(t)$ gives

$$L[R(t)/a_m a_n a_h] = \mu_0 + \frac{\sigma}{a_m a_n a_h} S(t), \tag{15}$$

for which the backward averaged form is

$$L[R_W(t)/a_m a_n a_h] = \mu_0 + \frac{\sigma}{a_m a_n a_h} S_W(t). \tag{16}$$

Recall that spiking was eventually observed in response to a noiseless effective step input, $R(t)=\mu_0+Z(t)$ and $L[Z]=a_m a_h a_n(\mu^*-\mu_0)$, when $\mu^* \approx 9.8$. This point can be more simply stated by eliminating $Z(t)$ in favor of $R(t)$ to find

$$L[R(t)/a_m a_h a_n] = \mu^* \tag{17}$$

subject to zero-initial conditions on the derivatives of $R(t)$ while $R(0)=\mu_0$. Now, spiking is observed in response to $R(t)$ where $L[R(t)/a_m a_h a_n]=\mu^*$, when $\mu^* \approx 9.8$. An extension of this point to the response to noisy forcing (16) is that spiking is observed when any backward local average of the noisy input, i.e., the right-hand side of Eq. (16), exceeds approximately 9.8. This basic idea underlies the following discussion which leads to a "competition between averages" for the average time to fire in response to noisy inputs $R(t)=\mu_0+\sigma Q(t)$.

The time to a first spike, $\tau(\mu_0,\mu^*)$ [Sec. II C and Fig. 5 caption], in response to an effective step input $R(t)$ that satisfies $L[R(t)/a_m a_h a_n]=\mu^*$ and zero-initial conditions save $R(0)=\mu_0$, is reduced as μ^* is increased beyond $\mu^* \approx 9.8$. Stated another way, the inverse of $\tau(\mu_0,\mu^*)$ for fixed μ_0, $\mu^*(\mu_0,\tau)$, is a variable barrier in that spiking is only observed when a given level μ^* is exceeded for at least a time τ. This concept of a variable barrier is extended to the calculation of the expected time to fire, $E[T]$, associated with noisy inputs (16) to the HH equations, i.e., spiking is observed in response to noisy inputs, $R(t)$, when any of the width W backward local averages of the effective input, equal to the right-hand side of Eq. (16), exceeds the barrier $\mu^*(\mu_0,W)$. Hence, each instant in time, t, has a group of averages running over windows of width $0<W<t$. When a member of these averages exceeds the barrier, $\mu^*(\mu_0,W)$, a spike occurs. Larger averaging windows, W, are weaker competitors but have lower barriers to exceed while shorter averaging windows have higher barriers. This tradeoff results in a competition between averages of the windows for contribution to a spike, where the "winners" tend to be intermediate windows.

The expected time to fire $E[T]$, Fig. 6, is computed from the HH equations and the competition model. The expected time to fire $E[T]$ in the HH equations, is found by Monte Carlo simulation where Eq. (2) is forced by $R(t)=\mu_0+\sigma Q(t)$ with $Q(t)$ taken from $L[Q]=S(t)$. The numerical solution of the HH equations is computed using a fourth-order Runge–Kutta solver while the expected time to spike, $E[T]$, is taken as the average of the times between 1001 spikes (each spike is localized to a voltage peak following a zero crossing). $E[T]$ is also found from the competition model using the average of the times between 1001 spikes. Here, a spike is assumed to occur after the exceedence of backward local averages of the effective input, i.e., the right-hand side of Eq. (16) equal to $\mu_0+\sigma/(a_m a_n a_h)S_W(t)$, over the barrier $\mu^*(\mu_0,W)$. Specifically, backward local averages are computed starting from $0<W<t$ until a first exceedence of the barrier is found at $t=t^*$. The backward averages are then reinitialized at the window $W=0$, and time $t=0$ is reset to the first sample beyond $t=t^*$. The backward local averages are then calculated from the "new" $t=0$ from $0<W<t$ until, as before, a first exceedence of the variable barrier is found. This yields a sequence of realizations of the minimum back-

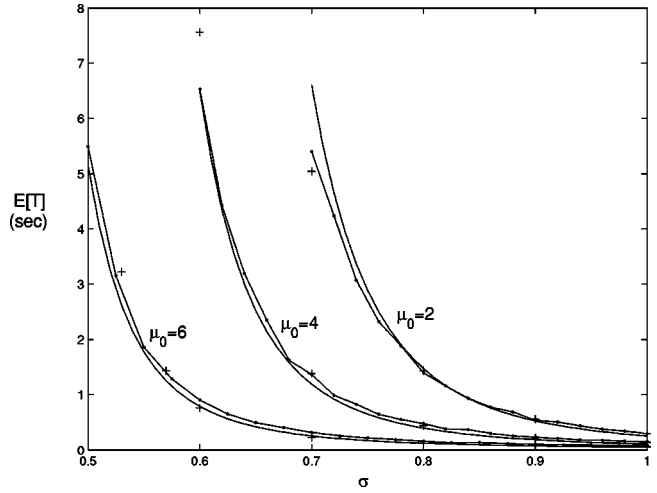

FIG. 6. The expected time to fire $E[T]$ is, respectively, depicted for $\mu_0=2$, $\mu_0=4$, and $\mu_0=6$ over $0<\sigma<0.5$ from: The competition model (solid line with dot markers, Sec. V), the HH equations ("+" symbols, Sec. II), and the energy model (solid line 18). These results show that the competition and its simplification closely describe the expected time to fire in the HH equations in response to red noise fluctuations defined in Ref. 15.

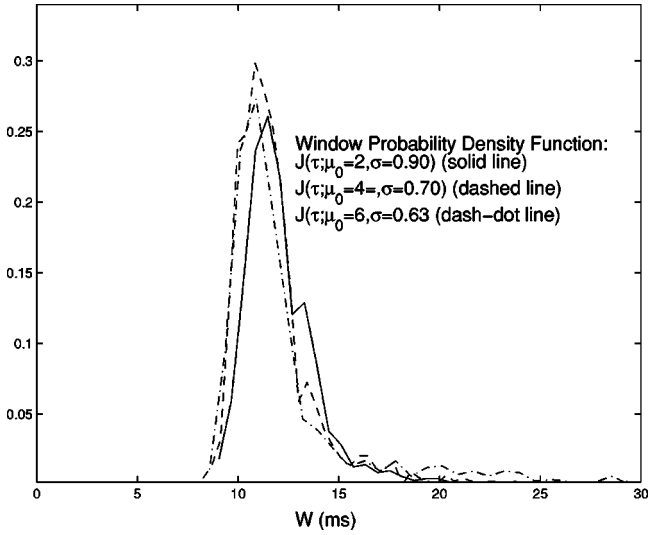

FIG. 7. The probability density function $J(W;\mu_0,\sigma)$ of the windows, W, responsible for spiking is shown for a range of μ_0. Intermediate windows on the order of 10 ms tend to "win" over competitors at shorter windows with higher barriers (Sec. IV) and those with longer windows but lower barriers.

ward local average width, W, required to achieve a spike. The barrier used in the competition is the inverse of $\tau(\mu_0,\mu^*)$, that is the wide lines shown in Fig. 5. Finally, the response predicted by the linearized HH equations in response to the step input is equal, as expected, to the order of that observed for the HH equations. However, to obtain the level of agreement between the competition model and the HH equations seen in Fig. 6, higher-order effects of nonlinearities present in the HH equations are modeled through a lumped parameter δ. Specifically, a constant scaling δ is applied to the standard deviation σ and, for example, at $\mu_0=2$ the results in Fig. 6 are achieved for the choice $\delta=1.35$. This means that the amplification of the noise level σ predicted by the linearized form, equal to $\sigma/a_m a_h a_n \approx 12\sigma$ in our example, is increased to reflect the effects of nonlinearities in the HH equations.

A representation of cause and effect between the noisy inputs $R(t)=\mu_0+\sigma Q(t)$ and spiking is contained in the probability density function, $J(W;\mu_0,\sigma)$, of the backward averaging windows, W, responsible for spiking. $J(W;\mu_0,\sigma)$ is shown in Fig. 7 for $\mu_0=(2,4,6)$. The probability density function shows little variation as a function of μ_0 with most of the window range confined to within ±2 ms of $\tau=10$ milliseconds. These results lead to a connection between the spectral content of the red noise inputs, $R(t)$, and the ion channel time constants. First, the external inputs $R(t)$ are whitened via the differential operator L, viz. the transfer function $H_S(\omega)$ (11) whose form is determined by the three ion channel time constants. Second, these inputs are backward averaged over a typical backward averaging window $\overline{W}$ equal to the order of the HH sodium channel activation time constant ($a_m \approx 4$ ms). Thus, the input power spectrum is first whitened and then low-pass filtered to reduce higher-frequency components beyond the sodium activation time scale. In summary, spiking is a mainly a response to spectral power of whitened inputs at frequencies corresponding to periods at or longer than the sodium channel activation time scale. With respect to control, based upon signals of the form of $R(t)$ (Sec. IV), the slowly varying control signal $\mu(t)$ is naturally distinguished from the superimposed fast fluctuations by the whitening process since it is less affected by the rapid increase of $H_S(\omega)$ for increasing ω.

V. SIMPLIFIED ENERGY MODEL

The spiking process may also be approximated by a point Poisson process since interspike intervals are approximately exponentially distributed and independent. Specifically, if the firing times, T, follow a Poisson point process then the backward moving average of the right-hand side of Eq. (15) over a fixed window U is a random function with an average time between upcrossings over a constant threshold $\overline{\mu}-\mu_0$ given by

$$q(\mu_0,\sigma)=\pi\sqrt{2\theta U}\,\exp\left\{\frac{(\overline{\mu}-\mu_0)^2 U}{2\sigma^2\theta}\right\}, \qquad (18)$$

when the window U greatly exceeds the correlation scale of fluctuation $\theta=0.5$ ms [26]. The closed-form approximation (18), based on the constant threshold $\overline{\mu}-\mu_0$ and constant window U, is compared to the competition results in Fig. 6. The constant windows, U, used in $q(\mu_0,\sigma)$ are set equal to the expected value of W, $\overline{W}$, previously found from the competition (Sec. IV). The constant barrier height, $\overline{\mu}$, is empirically chosen to produce the close comparison of the competition results with the constant barrier approximation seen in Fig. 6. The values of $\overline{\mu}$ used in Fig. 6 are within 10% of the variable barrier level evaluated at $\overline{\mu}$.

The closed-form energy formulation (18) is a constant barrier and constant averaging window approximation of the

competition. From this point of view, for inputs $R(t)=\mu+\sigma Q(t)$, a spike occurs on average when the linear combination of derivatives of the backward moving average of $R(t)$ taken over a constant window U, i.e., $L[R_W]$ (15), exceeds the constant barrier $\overline{W}-\mu_0$, where $\overline{W}$ is the order of the sodium time constant.

VI. DISCUSSION

Neurocardiology is the study of how the autonomic nervous system controls cardiac function to maintain sufficient blood flow throughout the body. Intriguing evidence of the promise for neurally based cardiac therapy comes from neurocardiological studies where electrical stimulation of the dorsal columns of the thoracic spinal cord has been shown to relieve symptoms associated with myocardial ischemia [19]. Such research requires better knowledge of the anatomic and functional organization of neurons controlling ischemic heart function.

To date, research into neural control of cardiac function broadly indicates two features: (i) A distributed neural network originating at the level of the heart that includes ganglia in the intrathoracic, spinal cord, and medullary regions, and is mainly involved in long-term (many beats) cardiac control [27,28]. This network may represent an important contribution to the development of the clinical condition of essential hypertension, a prevalent disorder in which patients express chronically elevated blood pressure without a clear pathophysiological explanation. (ii) Chemosensory feedback of heart status derived from fields of bare nerve endings that inervate the heart [19] is inherently noisy yet may be important to longer-term control.

The observation that spatially distributed networks of bare nerve endings (or sensory neurites) culminate in a many-to-one relationship at a cardiac afferent (feedback) neuron is important to the organization of neural control of cardiac function. Specifically, the observation was made here that the interspike intervals for such afferent neurons can be independent and approximately exponentially distributed. A simplified mathematical model for this sensory arrangement, that also approximates the observed distribution of interspike intervals, is the HH equations externally forced by subthreshold inputs perturbed by red noise. When interspike intervals are independent and approximately exponentially distributed, the response of the HH equations to external inputs may be characterized in terms of: (i) Their whitening of the input power spectrum (increase of input spectral power for increasing frequency), and (ii) their response to essentially those components with periods of fluctuation at or longer than the sodium activation timescale. Hence, inputs perturbed by red noises are whitened and from the point of view of control, the whitening is a means to distinguish the red noises from a slowly varying control signal.

In the competition energy model, only a fraction of the interspike interval is "responsible" for spiking since the inputs are deemed to *cause* spiking only when they exceed a barrier for a duration equal to the order of the sodium activation time scale. It is interesting to note that a similar concept (the competition energy model originally appeared in Ref. [29]) has also been explored, from a completely different point of view, for escape over a fluctuating barrier Ref. 30 (a nice review appears in Ref. [30]).

Combining the method used here to analyze the HH equations with the development of ion channel models for cardiac afferent neurons may prove useful to better understand neural processing of sensory neurite information. Another practical point relating to neurocardiological experiment, is that low pointwise correlation between cardiac afferent activity and observables, such as heart rate and blood pressure, should not be taken as an indication of the lack of relevance of neural activity.

ACKNOWLEDGMENTS

The authors wish to thank the Canadian National Science and Engineering Research Council for operating grant funds and a reviewer for comments leading to a clearer presentation.

[1] F. Moss, D. Pierson, and D. O'Gorman, Int. J. Bifurcation Chaos Appl. Sci. Eng. **4**, 1383 (1994).
[2] L. Gammaitoni, P. Hanggi, P. Jung, and F. Marchesoni, Rev. Mod. Phys. **70**, 223 (1998).
[3] J. J. Collins, C. C. Chow, A. C. Capela, and T. T. Imhoff, Phys. Rev. E **54**, 5575 (1996).
[4] C. Heneghan, C. C. Chow, J. J. Collins, T. T. Imhoff, S. B. Lowen, and M. C. Teich, Phys. Rev. E **54**, R2228 (1996).
[5] A. Capurro, K. Pakdaman, T. Nomura, and S. Sato, Phys. Rev. E **58**, 4820 (1998).
[6] A. Longtin, J. Stat. Phys. **70**, 309 (1993).
[7] B. Lindner and L. Schimansky-Geier, Phys. Rev. E **60**, 7270 (1999).
[8] S. R. Massanes and C. J. P. Vicente, Phys. Rev. E **59**, 4490 (1999).
[9] J. A. Armour, *Reflex Control of the Circulation* (CRC Press, Boca Raton, FL, 1991).
[10] J. C. G. Coleridge, A. Hemmingway, R. L. Holmes, and R. J. Linden, J. Physiol. (London) **136**, 174 (1957).
[11] H. M. Coleridge, J. C. G. Coleridge, and C. Kidd, J. Physiol. (London) **174**, 323 (1964).
[12] A. Malliani, Rev. Physiol. Biochem. Pharmacol. **94**, 11 (1982).
[13] A. S. Paintal, J. Physiol. (London) **120**, 596 (1953).
[14] G. W. Thompson, M. Horackova, and J. A. Armour, Can. J. Physiol. Pharmacol. **78**, 293 (2000).
[15] J. A. Armour, *Neurocardiology* (OUP, 1994).
[16] C. D. Lewis, G. L. Gebber, P. D. Larsen, and S. M. Barman, J. Neurophysiol. **85**, 1614 (2001).
[17] M. H. Huang, R. M. Negoescu, M. Horackova, S. Wolf, and J.

A. Armour, Cardiovasc. Res. **32**, 503 (1996).
[18] G. W. Thompson, M. Horackova, and J. A. Armour, Am. J. Physiol. **279**, R433 (2000).
[19] R. D. Foreman, R. W. Blair, H. R. Holmes, and J. A. Armour, Am. J. Physiol. **276** R976 (1999).
[20] M. C. Andresen and M. Yang, Clin. Exp. Pharmacol. Physiol. **15**, 19 (1989).
[21] J. A. Armour, Am. J. Physiol. **225**, 177 (1973).
[22] Z. Cheng, T. L. Powley, J. S. Schwaber, and F. J. Doyle, J. Comp. Neurol. **381**, 1 (1997).
[23] P. Thoren, Rev. Physiol. Biochem. Pharmacol. **86**, 1 (1979).
[24] J. O. Arndt, P. Brambling, K. Hindorf, and R. Rohnelt, J. Physiol. (London) **240**, 33 (1974).
[25] J. J. Collins, C. C. Chow, A. C. Capela, and T. T. Imhoff, Phys. Rev. E **54**, 5575 (1996).
[26] E. Vanmarcke, *Random Fields* (The MIT Press, Cambridge, MA, 1984).
[27] J. Lipski, J. Lin, M. Teo, and M. van Wyk, Auton. Neurosc.: Basic and Clinical **98**, 85 (2002).
[28] F. M. Smith, A. S. McGuirt, D. B. Hoover, J. Leger, J. A. Armour, and J. L. Ardell, Am. J. Physiol. **281**, H1919 (2001).
[29] G. C. Kember, G. A. Fenton, K. Collier, and J. A. Armour, Phys. Rev. E **61**, 1816 (2000).
[30] J. Iwaniszewski, I. K. Kaufman, P. V. E. McClintock, and A. J. McKane, Phys. Rev. E **61**, 1170 (2000).